Highly Anisotropic Glassy Polystyrenes Are Flexible

Huang, Qian; Madsen, Jeppe; Yu, Liyun; Borger, Anine; Johannsen, Sabrina Rostgaard; Mortensen, Kell; Hassager, Ole

Published in:
A C S Macro Letters

Link to article, DOI:
10.1021/acsmacrolett.8b00485

Publication date:
2018

Document Version
Peer reviewed version

Highly Anisotropic Glassy Polystyrenes Are Flexible

Qian Huang,*,† Jeppe Madsen,† Liyun Yu,† Anine Borger,‡ Sabrina Rostgaard Johannsen,§ Kell Mortensen,‡ and Ole Hassager†

†Department of Chemical and Biochemical Engineering, Technical University of Denmark, 2800 Lyngby, Denmark

‡Niels Bohr Institute, University of Copenhagen, 2100 Copenhagen, Denmark

§ DFM A/S, Danish National Metrology Institute, 2970 Hørsholm, Denmark

ABSTRACT: We show that stretching polystyrene melts at a rate faster than the inverse Rouse time followed by rapid quenching below the glass transition temperature, results in a material that is flexible and remains so for at least six months. Oriented micro/nano fibers are observed in the flexible samples after the mechanical tests. The fibers are probably related to the highly aligned molecules in melt stretching. At room temperature, a tensile strength over 300MPa has been achieved for the flexible polystyrenes.

Polymers above their glass transition temperatures (T_g) are known as viscoelastic materials. Below T_g, polymers typically show a reduction in ductility. A good example is polystyrene (PS), which is an amorphous material with a T_g around 100°C. At room temperature, it is hard and brittle. However, in contrast to PS, some amorphous polymers like polycarbonate (PC) are known as ductile polymers below T_g. The established model for analyzing the mechanical properties of glassy polymers is a two-component model originally proposed by Haward and Thackray [1]. In this model, the stress is decomposed into a contribution from intermolecular forces (secondary bonds) and a contribution from covalent bonding in the polymer network (primary bonds). The model has been used to explain the brittleness of PS and the toughness of PC [2-3]. PS ages faster than PC. It has a higher yield stress and a weaker hardening in stress-strain response than PC, and hence a stronger localization of strain (revealed as a pronounced strain softening). The strong localization results in the brittleness of PS. Interestingly, glassy PS may become flexible when compressed at room temperature in a two-roll milling process. This is known as mechanical rejuvenation, and has been studied in several papers [3-6]. The explanation is that the secondary bonds are locally weakened by compression, resulting in a reduced yield stress, and the strain localization is thus removed. However, the flexibility from mechanical rejuvenation is merely temporary. After a short time (typically minutes to hours for PS), brittleness returns. In this letter, we show that fast stretching of PS melts followed by rapid quenching below T_g leads to flexible PS. No brittleness is observed after half a year.

It is known that the processing history in liquid state influences the mechanical properties in solid state for polymers. For example, Zartman *et al.* [7] stretched a commercial PS at temperatures above T_g and subsequently quenched the samples below T_g. At room temperature, the resulting engineering stress of the quenched samples at fracture was up to 140 MPa, which is higher than values of 20-55 MPa reported for isotropic (without molecular alignment) glassy PS [8-9]. In the present work, we first also tested a commercial PS (see Supporting Information, SI). Sample A was slowly stretched at 160°C and allowed to relax in the melt state (so that the molecular conformation is isotropic) before cooling to room temperature. Sample B was stretched at 0.03 s^{-1} at 125°C to Hencky strain (see SI) 3.3, and subsequently quenched to the solid state without a relaxation step. Fig. 1a shows the results of the tensile tests at room temperature. Sample A fractured at a strain (see SI) of 1.3% with a tensile strength of 40MPa, while sample B fractured at a larger strain of about 33% with a tensile strength of 140 MPa. These values are consistent with the values reported by Zartman *et al.* [7]. The two samples have similar Young's modulus of 3-4 GPa. Fig. 1b shows the results of three-point bending tests. The Young's modulus obtained from the bending tests is consistent with the values obtained from the tensile tests. But the yield stress in the bending test is probably overestimated due to the use of linear elasticity (see SI). We observed that in both tensile and bending tests, Sample A fractured in a brittle manner with two flat surfaces. By contrast, Sample B fractured like a rope in the tensile test (Fig. 1a). Furthermore, removing Sample B from the bending test and subjecting it to further bending manually, the sample was surprisingly flexible, as shown in the photo in Fig. 1b.

Since Sample A is isotropic on the molecular scale, the flexibility of Sample B must be related to the molecular alignment. The question remains what degree of anisotropy leads to the flexibility. According to the classic tube theory [10-11] for entangled polymer liquids, molecular alignment includes both chain orientation and stretching.

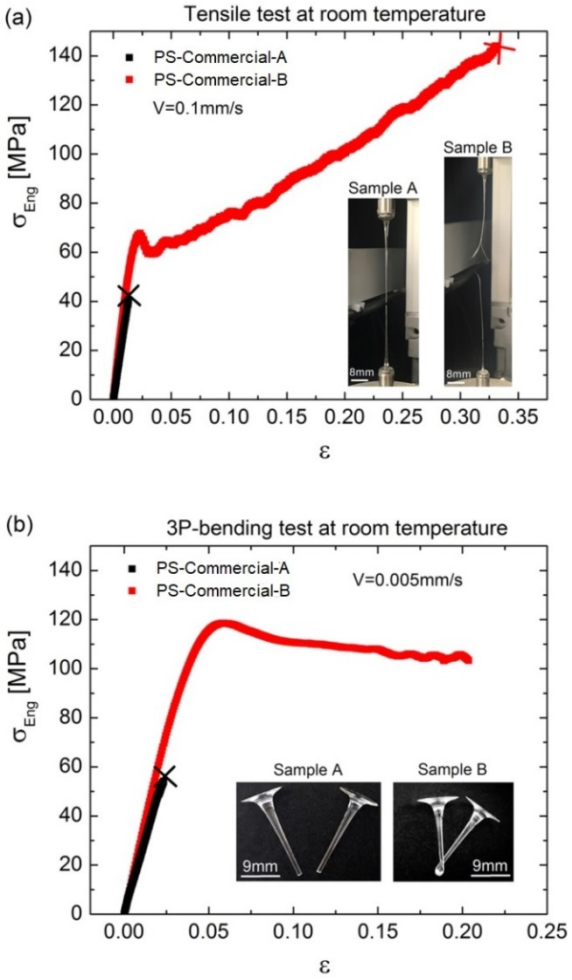

Figure 1. Engineering stress as a function of strain in (a) tensile tests, and (b) 3-point bending tests, at room temperature for PS-Commercial. Sample A is isotropic, while Sample B is an anisotropic sample with molecular alignment. The crosses represent the fracture points.

Chain orientation relaxes with the reptation time τ_d, while chain stretching relaxes with the Rouse time τ_R, with $\tau_R < \tau_d$. The τ_d and τ_R can be easily determined for monodisperse linear polymers, but it is not straightforward for polydisperse polymers (see SI). In order to investigate the critical condition, we tested a near-monodisperse PS-100k. We stretched two samples above T_g. PS-100k-A was stretched faster than $1/\tau_R$, leading to chain stretching. PS-100k-B was stretched slower than $1/\tau_R$ but faster than $1/\tau_d$, leading to chain *orientation* but not stretching. Both samples were stretched to a Hencky strain of 3.3 where the extensional stress reached a steady value, and subsequently quenched below T_g. At room temperature, PS-100k-A was flexible. However, PS-100k-B broke similarly to the isotropic commercial PS (see Fig. S3). We then stretched two more samples, PS-100k-C and PS-100k-D, at the same rate as PS-100k-A (*faster* than $1/\tau_R$). When the flow was stopped at Hencky strain 3.3, we allowed the samples to relax at 125°C. PS-100k-C was relaxed for 40s, which is *shorter* than τ_R, and then quenched. This sample was flexible like PS-100k-A. PS-100k-D was relaxed for 200s, which is longer than τ_R but shorter than τ_d. The resulting sample broke like PS-100k-B (See Fig. S4). The above observations show that molecular chain stretching is a key factor in inducing flexibility in the solid state.

But how does molecular chain stretching induce flexibility? The chain stretching corresponds to the network stretching in the Haward and Thackray model (i.e. the chain segments between entanglements are stretched). One possibility is that when the network is pre-stretched in the melt state, its contribution to stress in the solid state may dominate earlier in macroscopic strain. Therefore, the localization (strain softening) is removed by enhancing the contribution from the primary bonds (while in mechanical rejuvenation, it is removed by weakening the secondary bonds). However, it is also reported that fast stretching in melt state leads to loss of entanglements [12-13], which may also weaken the contribution from the network in solid state. On the other hand, it is reported that in melt stretching there is a chain orientation / stretching induced reduction of segmental friction [14-15]. According to Yaoita *et al.* [14], the segmental friction of PS melts starts decreasing sharply when stretched faster than $1/\tau_R$. Therefore, the reduced segmental friction may weaken the secondary bonds in solid state, similarly to mechanical rejuvenation.

Given the above results, we wondered if the right processing could lead to larger tensile strength for PS. Tensile strength of up to 140 MPa (engineering stress) for anisotropic PS has been reported by Zartman *et al.* [7]. The authors further reported that the tensile strength increased with the stretch rate and strain above T_g. Generally speaking, when a PS melt is stretched at a fixed rate above T_g, the transient stress increases with increasing strain, until a saturation value (steady stress) is reached [16-17], or an elastic fracture takes place [18]. Fig. 2a plots the steady stress as a function of stretch rate at 130°C for a near-monodisperse PS-285k. The critical stress at fracture is also plotted in the figure for faster stretch rates. If the larger stress in the melt stretching gives the larger tensile strength in the solid state, then the sample quenched near the highest critical stress in Fig. 2a should have the highest tensile strength. To test this hypothesis we quenched a sample of PS-285k near the highest critical stress (Sample B in Fig. 2a) and another sample at a lower stress (Sample A in Fig. 2a). Fig. 2b shows the results of the tensile tests for the corresponding quenched samples. A fully relaxed sample of PS-285k, with tensile strength 57 MPa, is also plotted in Fig. 2b for comparison. PS-285k-A fractured at an engineering stress of 175 MPa in the tensile test, while PS-285k-B reached 240 MPa. During the latter test, the load cell of the instrument was maxed out, and therefore we were unable to measure the tensile strength of PS-285k-B. But the achieved engineering stress of 240 MPa, corresponding to a true stress of about 300 MPa, is already higher than any reported values for glassy PS in literature.

Going back to the origin of flexibility as discussed above, compared with PS-285k-A, PS-285k-B has more molecular chain stretch in melt state [19-20], correspond-

ing to a more pre-stretched network, and possibly more reduction of segmental friction. However, unlike mechanical rejuvenation which lowers the yield stress, PS-285k-B has an even higher yield stress. And despite the possibility of losing entanglements, the strain hardening behavior after the yielding point is more pronounced, indicating an enhanced contribution from the network. It can also be seen that the strain-softening is almost fully erased for PS-285k-B. Therefore we make the hypothesis that, the origin of flexibility is loss of strain localization due to enhanced contribution of the stress from the pre-stretched network.

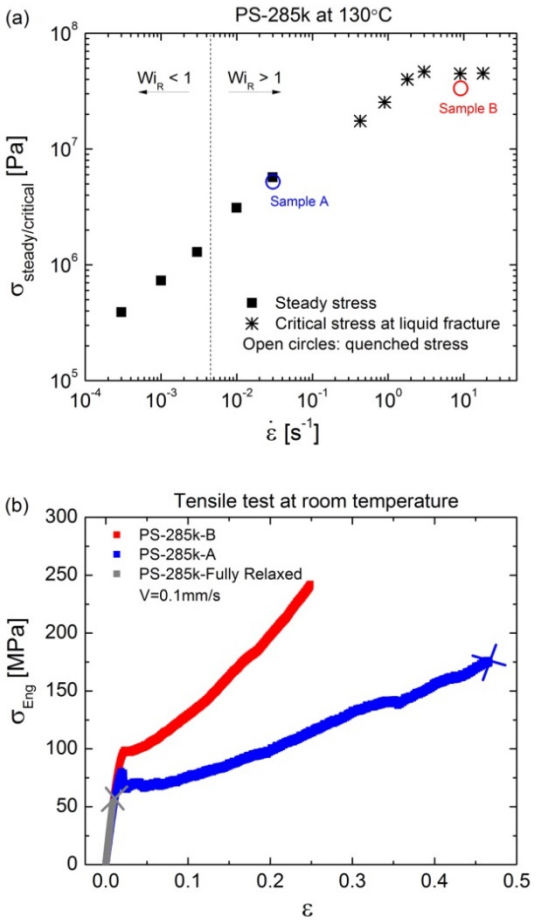

Figure 2. (a) Steady stress (taken from Ref. [17]) and critical stress at fracture as a function of stretch rate for PS-285k at 130°C. The Weissenberg number is defined as $Wi_R = \dot{\varepsilon}\tau_R$. (b) Engineering stress as a function of strain at room temperature for the quenched PS-285k samples.

We further checked the quenched flexible PS for signs of crystallization. Differential scanning calorimetry (DSC) curves show a relaxation exotherm for the highly anisotropic samples (see SI), but no sign of melting/ crystallization. Fig. 3 shows the wide angle X-ray scattering (WAXS) patterns for the flexible PS-100k-A (right) and the isotropic PS-100k (left). Crystallization is not observed from the patterns as expected from an atactic sample. The strain induced alignment is most clearly expressed in the correlation between neighboring chains (the inner ring). The 'isotropic' PS-100k sample shows only minor, if any, anisotropy (see also Fig. S7), thus proving the isotropic characteristics.

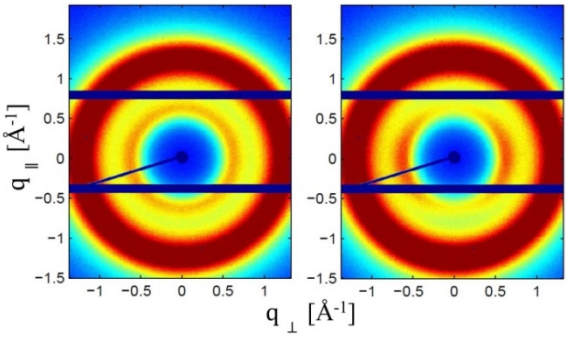

Figure 3. WAXS patterns for isotropic PS-100k (left) and flexible PS-100k-A (right).

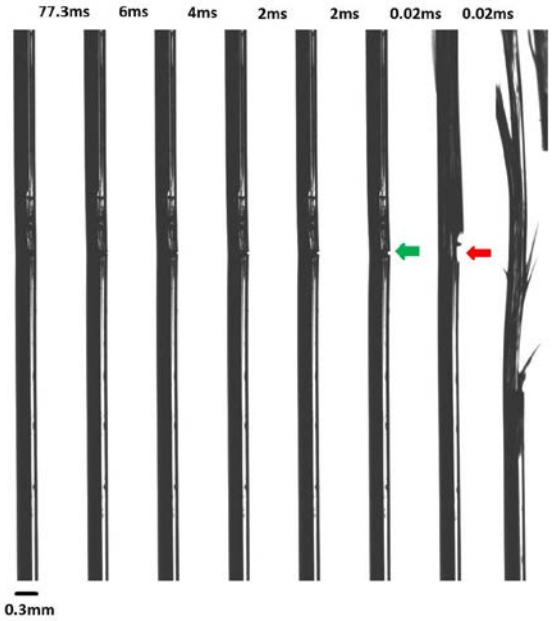

Figure 4. High-speed images taken at 50,000 frames per second showing the fracture process for PS-Commercial-B in the tensile test. The time between the adjacent frames are shown on the top. The green arrow marks a small crack with an approximate parabolic outline, and the red arrow shows that it changes to a sliding pattern.

Now we turn to the rope-like fracture. Fracture in isotropic PS glass is due to strain localization, leading to crazing [21] prior to fracture. This fracture corresponds to scission of the C-C bonds in the chain [22-23]. However, in contrast to the flat fracture surfaces of isotropic PS, we observed that the flexible samples *always* fractured into non-uniform fibers in tensile tests. Fig. 4 shows the images of PS-Commercial-B during the last 0.1s before fracture in the tensile test (in Fig. 1a). From the first 6 frames of Fig. 4 it can be seen that a small crack on the filament

surface (green arrow) is propagating with an approximate parabolic outline. However, this crack does not propagate throughout the entire cross section. Instead, the parabolic outline is replaced by a sliding pattern (red arrow) in a very short time of 0.02ms. In the final 0.02ms, additional sliding happens and the filament breaks at multiple sites, resulting in the rope-like fracture. The fracture surfaces of both flexible and brittle samples were investigated by optical microscopy. Fig. 5a and 5c show images for PS-Commercial-A and PS-Commercial-B, respectively. The flat surface after fracture is clearly seen for the brittle PS in Fig. 5a, meaning that unlike the case in Fig. 4, a crack has propagated throughout the cross section. The crazing phenomenon can also be clearly observed in Fig. 5a. In Fig. 5c, fibers are observed for the flexible sample. Fig. 5b and 5d show the corresponding scanning electron microscopy (SEM) images of the brittle and flexible samples, respectively. The oriented fiber structure is clearly seen in Fig. 5d, with multiple dimensions from micrometers to hundreds of nanometers (see also Fig. S8).

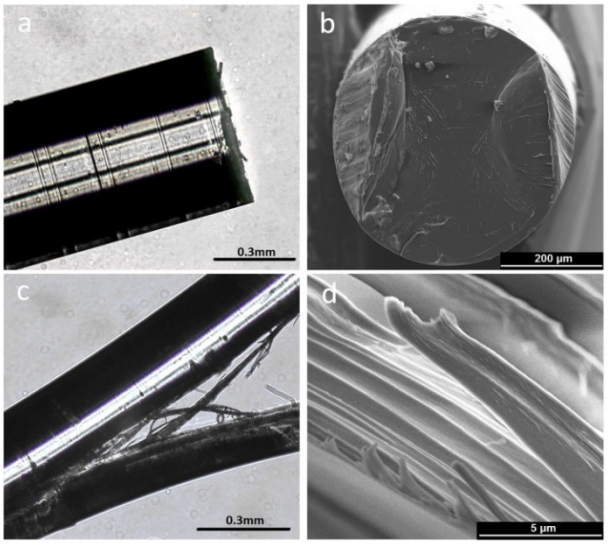

Figure 5. (a) Optical microscopy image and (b) SEM image, for the brittle sample PS-Commercial-A; (c) Optical microcopy image and (d) SEM image, for the flexible sample PS-Commercial-B.

Apparently, the oriented micro/nano fibers in Fig.5 and the stop of crack propagation in Fig.4 are the key factors leading to the rope-like fracture. But why does the crack stop growing? After fracture in tensile tests, most part of the broken filament was still transparent, except the part near the fracture place. Fig. 6 shows the SEM images of the transparent part that have been embedded in epoxy and microtomed both perpendicular to and along the tensile stretching direction. Cracks propagating the sample with a width below 100 nm, can be seen in the cross section perpendicular to the stretching direction. This is also confirmed in the atomic force microscopy (see Fig. S9). Along the stretching direction, discrete structures with a length scale on the order of 100 nm can be seen. This is confirmed by the high transparency of the stretched filaments, which indicate that any intrinsic structures are significantly smaller than the wavelength of visible light. Based on these results, we make the hypothesis that, the crack in Fig. 4 stops propagating along the direction perpendicular to the stretching, because the crack tip meets an elongated void. When this happens, the crack deflects along the direction of lowest fracture toughness leading to fibrillation.

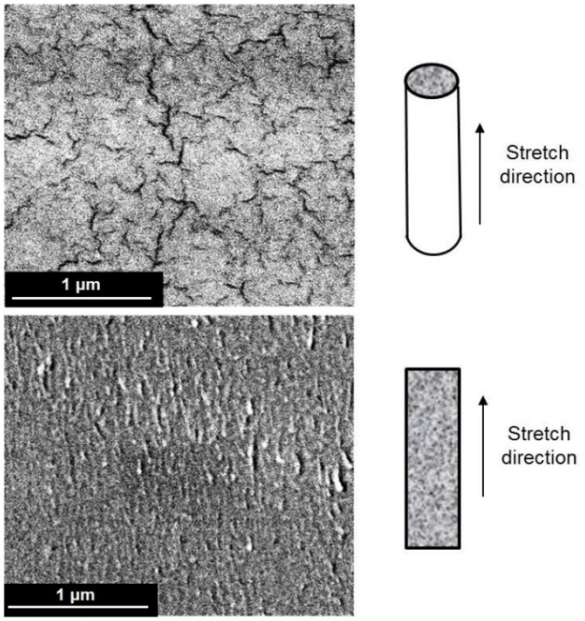

Figure 6. SEM images of microtomed cross sections perpendicular to (top) and along (bottom) the tensile stretching direction, for the flexible sample PS-Commercial-B (shown in Fig. 1a).

In summary, we have shown that glassy PS can become flexible by stretching the melts above T_g at a rate faster than the inverse Rouse time and subsequently quenching to the solid state. The flexibility is probably due to loss of strain localization by enhancing the contribution of stress from the polymer network. Oriented micro/nano fibers have been observed in the flexible samples after fracture or microtoming. The fibrous structure probably originates from the highly aligned molecules in the melt due to fast stretching. Interestingly, in a recent publication [24], the oriented nanofiber structures are also observed in the densified wood, which also gives a much larger tensile strength than the normal wood. Flexible, transparent PS with improved tensile strength may have applications such as optical fibers, while the manufacturing process is likely to be transferable to other polymers, thereby leading to a general method for preparing stronger materials.

ASSOCIATED CONTENT

Supporting Information

Materials, experimental details, and supporting figures. This material is available free of charge via the Internet at http://pubs.acs.org.

AUTHOR INFORMATION

Corresponding Author

*E-mail: qh@kt.dtu.dk

Notes

The authors declare no competing financial interest.

ACKNOWLEDGMENT

Financial support from the Aage og Johanne Louis-Hansen Foundation is gratefully acknowledged. We thank Lars Schulte from DTU Nanotech for microtoming the samples. We thank Prof. Gerrit W. M. Peters and Prof. Leon E. Govaert from Eindhoven University of Technology, and Dr. Tom Engels from DSM for constructive comments and discussions on mechanical rejuvenation and crazing of polystyrenes. We would also like to thank the three anonymous reviewers for their valuable comments.

REFERENCE

(1) Haward, R. N.; Thackray, G. The Use of a Mathematical Model to Describe Isothermal Stress-Strain Curves in Glassy Thermoplastics. *Proc. Roy. Soc.* **1968**, A. 302, 453–472.

(2) Smit, R. J. M.; Brekelmans, W. A. M.; Meijer, H. E. H. Predictive Modelling of the Properties and Toughness of Polymeric Materials - Part I Why is Polystyrene Brittle and Polycarbonate Tough. *Journal of Materials Science* **2000**, 35, 2855–2867.

(3) Meijer, H. E. H.; Govaert, L. E. Mechanical Performance of Polymer Systems: The Relation between Structure and Properties. *Progress in Polymer Science* **2005**, 30, 915–938.

(4) Govaert, L. E.; Melick, H. G. H. van.; Meijer, H. E. H. Temporary Toughening of Polystyrene through Mechanical Pre-conditioning. *Polymer* **2001**, 42, 1271–1274.

(5) Melick, H. G. H. van.; Govaert, L. E.; Raas, B.; Nauta, W. J.; Meijer, H. E. H. Kinetics of Ageing and Re-embrittlement of Mechanically Rejuvenated Polystyrene. *Polymer* **2003**, 44, 1171–1179.

(6) McKenna, G. B. Mechanical Rejuvenation in Polymer Glasses: Fact or Fallacy. *Journal of Physics: Condensed Matter* **2003**, 15, S737–S763.

(7) Zartman, G. D.; Cheng, S.; Li, X.; Lin, F.; Becker, M. L.; Wang, S-Q. How Melt-stretching Affects Mechanical Behavior of Polymer Glasses. *Macromolecules* **2012**, 45, 6719–6732.

(8) Fried, J. R. *Polymer Science and Technology* (*third edition)*; Prentice Hall, 2014

(9) Jiang, S.; Duan, G.; Zussman, E.; Greiner, A.; Agarwal, S. Highly Flexible and Tough Concentric Triaxial Polystyrene Fibers. *ACS Applied Materials & Interfaces* **2014**, 6, 5918–5923.

(10) De Gennes, P. G. *Scaling Concepts in Polymer Physics*; Cornell Univ. Press: New York, 1979.

(11) Doi, M.; Edwards, S. F. *The Theory of Polymer Dynamics*; Clarendon Press, Oxford, 1986.

(12) Kushwaha, A.; Shaqfeh, E. S. G. Slip-link Simulations of Entangled Polymers in Planar Extensional Flow: Disentanglement Modified Extensional Thinning. *Journal of Rheology* **2011**, 55, 463–483.

(13) Schieber, J. D.; Nair, D. M.; Kitkrailard, T. Comprehensive Comparisons with Nonlinear Flow Data of a Consistently Unconstrained Brownian Slip-link Model. *Journal of Rheology* **2007**, 51, 1111–1141.

(14) Yaoita, T.; Isaki, T.; Masubuchi, Y.; Watanabe, H.; Ianniruberto, G.; Marrucci, G. Primitive Chain Network Simulation of Elongational Flows of Entangled Linear Chains: Stretch/Orientation-induced Reduction of Monomeric Friction. *Macromolecules* **2012**, 45, 2773–2782.

(15) Ianniruberto, G.; Brasiello, A.; Marrucci, G. Simulations of Fast Shear Flows of PS Oligomers Confirm Monomeric Friction Reduction in Fast Elongational Flows of Monodisperse PS Melts As Indicated by Rheooptical Data. *Macromolecules* **2012**, 45, 8058–8066.

(16) Bach, A.; Almdal, K.; Rasmussen, H. K.; Hassager, O. Elongational Viscosity of Narrow Molar Mass Distribution Polystyrene. *Macromolecules* **2003**, 36, 5174–5179.

(17) Huang, Q.; Mednova, O.; Rasmussen, H. K.; Alvarez, N. J.; Skov, A. L.; Almdal, K.; Hassager, O. Concentrated Polymer Solutions are Different from Melts: Role of Entanglement Molecular Weight. *Macromolecules* **2013**, 46, 5026–5035.

(18) Huang, Q.; Alvarez, N. J.; Shabbir, A.; Hassager, O. Multiple Cracks Propagate Simultaneously in Polymer Liquids in Tension. *Physical Review Letters* **2016**, 117, 087801.

(19) Hassager, O.; Mortensen, K.; Bach, A.; Almdal, K.; Rasmussen, H. K.; Pyckhout-Hintzen, W. Stress and Neutron Scattering Measurements on Linear Polymer Melts Undergoing Steady Elongational Flow. *Rheologica Acta* **2012**, 51, 385–394.

(20) Wagner, M. H.; Narimissa, E.; Huang, Q. On the Origin of Brittle Fracture of Entangled Polymer Solutions and Melts. *Journal of Rheology* **2018**, 62, 221–233.

(21) Fellers, J. F.; Kee, B. F. Crazing Studies of Polystyrene. I. A New Phenomenological Observation. *Journal of Applied Polymer Science* **1974**, 18, 2355–2365.

(22) Kramer, E. J. Microscopic and Molecular Fundamentals of Crazing. In: Kausch, H. H. (eds) *Crazing in Polymers. Advances in Polymer Science* 52-53, Springer, Berlin, Heidelberg, 1983.

(23) De Focatiis, D. S. A.; Buckley, C. P.; Hutchings, L. R. Roles of Chain Length, Chain Architecture, and Time in the Initiation of Visible Crazes in Polystyrene. *Macromolecules* **2008**, 41, 4484–4491.

(24) Song, J.; Chen, C.; Zhu, S.; Zhu, M.; Dai, J.; Ray, U.; Li, Y-J.; Kuang, Y.; Li, Y-F.; Quispe, N.; Yao, Y.; Gong, A.; Leiste, U. H.; Bruck, H. A.; Zhu, J. Y.; Vellore, A.; Li, H.; Minus, M. L.; Jia, Z.; Martini, A.; Li, T.; Hu, L. Processing Bulk Natural Wood into a High-performance Structural Material. *Nature* **2018**, 554, 224–228.